Contents lists available at ScienceDirect

Chemosphere

Australian Black summer smoke signal on Antarctic aerosol collected between New Zealand and the Ross sea

Elisa Scalabrin [a,b,*], Elena Barbaro [a,b], Sarah Pizzini [c,b], Marta Radaelli [b], Matteo Feltracco [b], Rossano Piazza [b], Andrea Gambaro [b,a], Gabriele Capodaglio [b]

[a] Institute of Polar Sciences, National Research Council (CNR-ISP), Via Torino, 155, 30172, Venice Mestre (VE), Italy
[b] Department of Environmental Sciences, Informatics and Statistics, Ca' Foscari University of Venice, Via Torino, 155, 30172, Venice Mestre (VE), Italy
[c] Institute for Marine Biological Resources and Biotechnology, National Research Council (CNR-IRBIM), Largo Fiera della Pesca, 2, 60125, Ancona, Italy

HIGHLIGHTS

- Biogenic and BB tracers in aerosol from the Southern Ocean were assessed.
- BB tracers were ten times higher than their mean values in Antarctic marine aerosol.
- Australian Black Summer wildfires influenced Antarctic aerosol composition.
- PAHs were only partially related to BB event, also having other regional sources.
- Increased frequency of wildfires may impact Antarctic aerosol radiative properties.

GRAPHICAL ABSTRACT
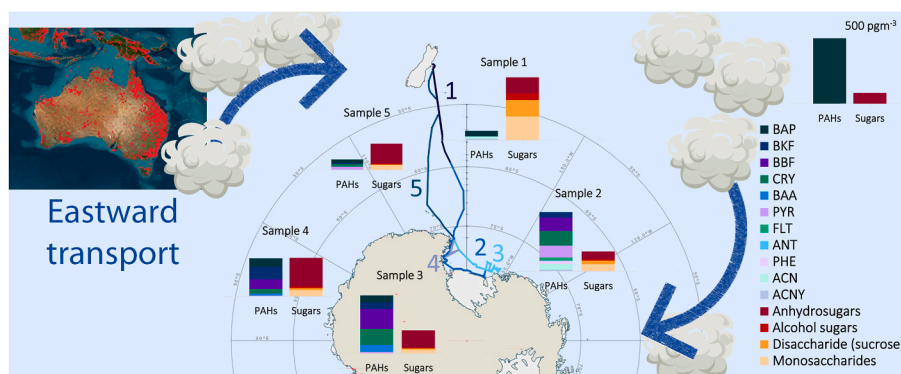
ARTICLE INFO

ABSTRACT

Open biomass burning (BB) events are a well-known primary aerosol source, resulting in the emission of significant amount of gaseous and particulate matter and affecting Earth's radiation budget. The 2019–2020 summer, known as "Australian Black Summer", showed exceptional duration and intensity of seasonal wildfires, triggered by high temperatures and severe droughts. Since increasing megafires are predicted due to expected climate changes, it is critical to study the impact of BB aerosol on a large scale and evaluate related transport processes. In this study, five aerosol samples (total suspended particles with a diameter >1 μm) were collected during the XXXV Italian Expedition in Antarctica on board of the R/V Laura Bassi from 6th of January to February 16, 2020, along the sailing route from Lyttelton harbor (New Zealand) to Terra Nova Bay (Antarctica). Levoglucosan and its isomers have been analyzed as markers of BB, together with polycyclic aromatic hydrocarbons (PAHs), sucrose and alcohol sugars. Ionic species and carboxylic acids have been analyzed to support the identification of aerosol sources and its aging. Results showed high levoglucosan concentrations (325–1266 pg m^{-3}) during the campaign, suggesting the widespread presence of smoke in the region, because of huge wildfire releases. Backward trajectories indicated the presence of long-range atmospheric transport from South America, probably carrying wildfires plume, in agreement with literature. Regional sources have been suggested for PAHs,

* Corresponding author.
  E-mail address: elisa.scalabrin@cnr.it (E. Scalabrin).

particularly for 3–4 rings' compounds; monosaccharides, sucrose, arabitol, and mannitol were related to marine and biogenic contributions. In a warming climate scenario, more frequent and extensive wildfire episodes are expected in Australia, potentially altering albedo, aerosol radiative properties, and cloud interactions. Therefore, it is crucial to strengthens the investigations on the regional climatic effects of these events in Antarctica.

1. Introduction

Biomass burning (BB) has been recognized as the largest source of primary fine carbonaceous particles, influencing the climate system and the Earth's solar balance (Carmichael et al., 2009; IPCC, 2021).

BB aerosol originates from the combustion of living and dead vegetation, including wildfires, prescribed burning, and domestic bio-fuel combustion (Cheng et al., 2013) and it is globally widespread, since it may be subject to long-range atmospheric transport (LRAT), reaching even remote and polar areas (Barbaro et al., 2015; Cao et al., 2018; Feltracco et al., 2020; Shi et al., 2019; Zangrando et al., 2016a). Australian open BB events, especially summer wildfires, are known to impact Antarctic atmosphere, with a relatively larger contribution in comparison to South America emissions (Stohl and Sodemann, 2010). The stratospheric trapping of Australian wildfire smoke above the Antarctic area has been observed after the 2009 summer season, and a ground-level impact over long time scales has been hypothesized (Jumelet et al., 2020).

The 2019–2020 wildfire season in Australia, also known as Australian Black Summer, was incomparable in terms of burned forest area, especially in the South-East of the country (Bowman et al., 2020; Jager and Coutant, 2020). It caused harmful levels of air pollution in many cities (Levin et al., 2021; Ryan et al., 2021) and destroyed the habitats of several types of Australian fauna (Khan, 2021). Wildfire smoke travelled thousands of kilometers in the stratosphere reaching South America (Ohneiser et al., 2020), also leading to anomalously widespread phytoplankton blooms from December 2019 to March 2020 in the Southern Ocean, triggered by Australian fire aerosol fertilization (Tang et al., 2021). The huge amount of emitted smoke has also been transported southward in the stratosphere, influencing stratospheric temperature over Antarctica and aerosol optical properties (Damany-Pearce et al., 2022; Simmons et al., 2022; Tencé et al., 2022).

Recent studies highlighted an increased frequency of Australian megafires (>10,000 km^2 of burned area) in the last two decades, triggered by increased temperatures and alterations in rainfall patterns (Canadell et al., 2021). Under this global changing scenario, extreme fire weather conditions are expected (Jain et al., 2022), with the related increased risk of extensive wildfire events (Yu et al., 2020). It is therefore crucial to understand the impact of such extreme BB event in a key-region as Antarctica, where increased organic aerosol input may highly affect aerosol radiative properties and its ability to act as cloud condensation nuclei (Novakov and Corrigan, 1996), increasing atmospheric energy storage (Ramanathan and Carmichael, 2008) and influencing snow albedo (IPCC, 2021). In addition, due to the limited local anthropogenic and BB sources and the surrounding oceans, Antarctica represent an ideal laboratory to study atmospheric aerosol sources, the role of aerosol markers in relation to different sources (biogenic, crustal, anthropogenic, secondary) and contaminant transport pattern from mid-latitudes. Improve the knowledge about carbonaceous aerosol transport toward Antarctica is particularly important to understand the contribution of BB source to the global Antarctic aerosol budget.

Among the BB organic tracers, levoglucosan, together with its isomers mannosan and galactosan, is widely recognized as a key-marker of biomass combustion, due to its specificity and high emission factors (Hu et al., 2013; Oros et al., 2006; Oros and Simoneit, 2001). Levoglucosan has been extensively applied in many studies carried out in continental, coastal, and remote regions (Chen et al., 2013; Hu et al., 2013; Nirmalkar et al., 2015; Sang et al., 2013; Simoneit et al., 2004). Polycyclic aromatic hydrocarbons (PAHs) are organic compounds originating from anthropogenic emissions such as combustion of fossil fuels, petrogenic releases, and BB, as well as by natural and biological sources (Cabrerizo et al., 2014; Zhang et al., 2021). PAHs are typically produced during incomplete combustion processes under oxygen deficient conditions and are known to be present in wildfire smoke (Kieta et al., 2023; Yuan et al., 2008).

The analysis of ionic species and of carboxylic acids can support the identification of aerosol sources and highlight the presence of aerosol aging processes (Barbaro et al., 2016a, 2017a; Fu et al., 2009), useful in the discrimination between LRAT mechanisms and primary regional sources.

In this work, levoglucosan and PAHs were determined, together with other complementary tracers, in aerosol samples collected during the XXXV Italian Expedition in Antarctica, on board of the R/V Laura Bassi during its trip from the Lyttelton harbor (New Zealand) to Terra Nova Bay (Antarctica), at the end of the Australian Black Summer, from 6th of January to February 16, 2020. The aim of the study was to identify major aerosol sources in the Southern Ocean and, particularly, in the Ross Sea, highlighting the presence of BB aerosol to unravel the impact of Australian megafires in this region. The biogenic input has been also evaluated by sugars (monosaccharides, disaccharides and alcohol sugars) and methanesulfonic acid (MSA) which is one of the major dimethylsulfide (DMS) oxidation products in atmosphere and is a tracer of phytoplanktonic emissions (Becagli et al., 2022). The evaluation of different aerosol sources (biogenic, crustal, anthropogenic) and of aerosol aging, by using suitable markers, was essential to discriminate the contribution of BB source and obtain information about aerosol origin in the Antarctica region. To our knowledge, this is the first study highlighting the presence of Australian wildfire smoke in the Antarctic troposphere.

2. Materials and methods

2.1. Sample collection

Total suspended particles (TSP) with a diameter >1 μm were collected on a circular quartz fiber filter (Filter-Lab, Filtros Anoia S.A., Spain), using a TE-5000 TSP High Volume Air Sampler (Tisch Environmental Inc., OH, USA). A wind control system (WindSonic ultrasonic wind sensor, Gill Instruments Ltd., UK) was used to avoid contamination from the ship, sampling only when wind direction was from bow with a speed higher than 1 m s^{-1}. For this reason, sampled air volumes varied between 1461 and 3415 m^3 and sampling time lasted from 2 to 7 days (Table S1). Sampling was conducted from the Lyttelton harbor (New Zealand) to Terra Nova Bay (Antarctica) from 6th of January to February 16, 2020. Before sampling, the quartz fiber filters were thermally cleaned at 400 °C for 4 h in a muffle furnace and then wrapped in aluminum foils. Prior to the start of the oceanographic campaign, a field blank was collected by loading in the sampling module a pre-cleaned quartz fiber filter, with the air pump switched off. After sampling, both blank and samples were folded and wrapped in aluminum foils and stored at −20 °C until analysis. Blank levels resulted similar to concentrations reported in method validation description during previous Antarctic campaigns (Barbaro et al., 2017a, Barbaro et al., 2015; Piazza et al., 2013) and were subtracted to the samples. The MDL and MQL were considered the same already assessed during validation.

2.2. Determination of sugars, ionic species, and carboxylic acids

Sample treatment procedure for the analysis of sugars (levoglucosan, galactosan, mannosan, arabinose, ribose, xylose, fructose, galactose, glucose, mannose, sucrose, erythritol, arabitol, xylitol, ribitol, mannitol, sorbitol, and maltitol), ionic species, and C_1–C_7 carboxylic acids (C_1-formic, C_2-acetic, C_2-glycolic, C_2-oxalic, C_3-malonic, C_4-succinic, hydroxy-C_4-malic, *cis*-C_4-maleic, *trans*-C_4-fumaric, C_5-glutaric, C_6-adipic, C_7-pimelic acids) was carried out as already described in Barbaro et al., 2020, Barbaro et al., 2015).

A quarter of each filter was spiked with a known amount of $^{13}C_6$-levoglucosan standard solution (CIL, Cambridge Isotope Laboratories Inc., MA, USA), ultrasonically extracted with ultrapure water (18.2 MΩ cm resistivity at 25 °C, 1 µg L^{-1} Total Organic Carbon), produced using a Purelab Ultra System (Elga LabWater - Veolia Water VWS Ltd., UK). The extracts were then filtered through a 0.45 µm PTFE filter.

Instrumental analysis of sugars was performed using a High-Performance Anion Exchange Chromatograph (HPAEC) Dionex ICS-5000 Ion Chromatography System, coupled with a TSQ Altis™ triple-quadrupole tandem Mass Spectrometer (MS/MS) system, equipped with a Heated-ElectroSpray Ionization (H-ESI) source (Thermo Fisher Scientific Dionex Inc., MA, USA) operating in negative mode (Barbaro et al., 2015). Separation was carried out with a CarboPac™ MA1 analytical column (250 mm length, 2 mm I.D.) coupled with an AminoTrap™ guard column (50 mm length, 2 mm I.D.), and with a CarboPac™ PA10 analytical column (250 mm length, 2 mm I.D.) coupled with a CarboPac™ PA10 guard column (50 mm length, 2 mm I.D.; Thermo Fisher Scientific Dionex Inc.). The injection volume was 50 µL. Acquisition was performed using Single Reaction Monitoring (SRM) mode while quantification was carried out using internal standard and the isotopic dilution technique. Results were corrected using the instrumental response factors and blank levels were evaluated and subtracted.

Instrumental analysis of anionic species (Cl$^-$, Br$^-$, I$^-$, NO$_3^-$, SO$_4^{2-}$, and MSA) and carboxylic acids was performed using the same Ion Chromatograph (IC), coupled with a single-quadrupole MSQ Plus™ MS system, equipped with a ESI source (Thermo Fisher Scientific Inc.) operating in negative mode, following the method described in Barbaro et al. (2019). Separation was carried out with an IonPac™ AS19 analytical column (250 mm length, 2 mm I.D.) coupled with an IonPac™ AG19 guard column (50 mm length, 2 mm I.D.; Thermo Fisher Scientific Dionex Inc.). Sodium hydroxide (NaOH) was used as mobile phase and was produced by a Dionex ICS-5000EG eluent generator (Thermo Fisher Scientific Inc.) with a flow rate of 0.25 mL min^{-1}. The injection volume was 100 µL. Acquisition was performed using Selected Ion Monitoring (SIM) mode while quantification was carried out using the external calibration curve technique. Results were corrected using the instrumental response factors and blank levels were evaluated and subtracted.

Instrumental analysis of cationic species (Na$^+$, Mg^{2+}, K$^+$, Ca^{2+}, and NH$_4^+$) was performed using the same IC, coupled with a conductivity detector (Thermo Fisher Scientific Inc.), as described in (Barbaro et al., 2019). Separation was carried out with an IonPac™ CS19-4 µm capillary cation-exchange column (250 mm length, 0.4 mm I.D.) coupled with an IonPac™ CG19-4 µm guard column (50 mm length, 0.4 mm I.D.; Thermo Fisher Scientific Dionex Inc.). MSA was used as mobile phase and was produced by a Dionex ICS-5000EG eluent generator (Thermo Fisher Scientific Inc.) with a flow rate of 13 µL min^{-1}. The injection volume was 0.4 µL. Quantification was carried out using the external calibration curve technique. Blank levels were evaluated and subtracted.

2.3. Determination of PAHs

Fifteen of the sixteen US EPA (Environmental Protection Agency) priority PAHs (*i.e.* ACNY: acenaphthylene; ACN: acenaphthene; FLU: fluorene; PHE: phenanthrene; ANT: anthracene; FLT: fluoranthene; PYR: pyrene; BAA: benz[*a*]anthracene; CRY: chrysene; BBF: benzo[*b*]fluoranthene; BKF: benzo[*k*]fluoranthene; BAP: benzo[*a*]pyrene; BPER: benzo[*ghi*]perylene; IPYR: indeno[1,2,3-*cd*]pyrene; DAHA: dibenz[*a,h*] anthracene) were analyzed following the pre-analytical procedure described in Piazza et al., 2013.

Half of each filter was broken into small pieces, mixed with diatomaceous earth (Applied Separations Inc., PA, USA), de-humidified with anhydrous sodium sulfate (Sigma-Aldrich Co., MO, USA), then placed in a 20 mL stainless steel extraction cell, spiked with a known amount of ^{13}C isotope-labeled standards ($^{13}C_6$-ACNY, $^{13}C_6$-PHE, and $^{13}C_4$-BAP at 1 ng µL^{-1}; CIL Inc., MA, USA), and covered with Ottawa sand (Applied Separations Inc.). Analyte extraction was carried out with an ASE™ 350 system (Accelerated Solvent Extractor; Thermo Fisher Scientific Dionex Inc.) at 100 bar and 100 °C in three cycles of 5 min each, using *n*-hexane-dichloromethane (1:1; v/v) as extracting solvent. The extracts were then reduced to 500 µL under a gentle nitrogen flow at 23 °C (Turbovap® II; Caliper Life Science Inc., MA, USA). The samples were then made up to 2 mL with *n*-hexane to change solvent and transferred into a glass syringe for injection into the automated clean-up system Power-Prep™ (FMS, Fluid Management System Inc., MA, USA). Clean-up was performed by directly injecting the sample into a disposable neutral silica column (19.5 × 0.9 cm with 6 g of silica; FMS Inc.), previously conditioned with 50 mL of *n*-hexane. Elution was carried out with 30 mL of *n*-hexane followed by 30 mL of *n*-hexane-dichloromethane (1:1; v/v). The eluates were collected as one single fraction. Sample volume was then reduced again to 100 µL and spiked with a known amount of the recovery standard $^{13}C_6$-CRY at 1 ng µL^{-1} (CIL Inc.).

Instrumental determination of PAHs was carried out following the method described by Pizzini et al., 2016), by means of a single-quadrupole Low-Resolution Mass Spectrometer (LRMS) Agilent Technologies 5973 inert Mass Selective Detector System, operating in Electron Ionization (EI) mode, coupled with a Gas Chromatograph (GC) Hewlett Packard - Agilent Technologies 6890 Series GC System, equipped with a HP5-ms column (30 m length, 0.25 mm I.D., 0.25 µm film thickness; Agilent Technologies Inc., CA, USA). Acquisition was performed using SIM mode while quantification was carried out using internal standards and the isotopic dilution technique. Results were corrected using the instrumental response factors and blank levels were evaluated and subtracted.

2.4. Statistical analysis

Hierarchical cluster analysis (HCA) was carried out using the StatSoft Inc. software Statistica 8.0, using Ward's method and Euclidean distance as clustering criteria. Ionic source apportionment calculation was performed on the basis of a previous study by Udisti et al. (2016) and chloride depletion was calculated as previously described by (Su et al., 2022). Backward trajectories have been calculated using the US NOAA (National Oceanic and Atmospheric Administration) HYSPLIT (Hybrid Single-Particle Lagrangian Integrated Trajectory) Trajectory Model (Rolph et al., 2017; Stein et al., 2015). GDAS (Global Data Assimilation System) meteorological database at one degree of resolution has been used, with the model vertical velocity as vertical motion option. For LRAT evaluation, seven days (168 h) back trajectories were calculated at 250, 500, and 1500 m AGL. To evaluate regional sources, daily 120 h back trajectories have been computed at 10, 50, and 250 m AGL, considering conventionally as ending point the position of the ship at 20:00 UTC every sampling day. To provide an estimation of phytoplanktonic biomass, 8 days Chlorophyll-*a* concentrations at 0.1 degree of resolution were obtained from the MODIS (Moderate-resolution Imaging Spectroradiometer) sensor on the NASA (National Aeronautics and Space Administration) Aqua satellite (EOS, Earth Observing System PM-1) and displayed (Level-3; OCI, Ocean Color Imager algorithm) with the Google LLC. software Google Earth.

3. Results

3.1. Sugars

All the considered sugar compounds, excluding ribitol, were detected in aerosol samples. The highest concentration was that of levoglucosan (325–1266 pg m^{-3}), followed by sucrose (32–756 pg m^{-3}), glucose (68–617 pg m^{-3}), and fructose (62–351 pg m^{-3}). The highest overall sugar content was observed in sample 1 (Fig. 1), with a total sugar concentration of 2873 pg m^{-3}; sucrose turned out to be its major component (26%), followed by levoglucosan (24%) and glucose (22%). The other samples had significantly lower total sugar content, ranging from 908 to 1760 pg m^{-3}. Sample 2 composition showed contributions from levoglucosan (35%), glucose (21%), and sucrose (19%). Instead, in samples 3, 4, and 5 levoglucosan was dominant sugar, with similar relative abundances of ≈72%.

3.2. PAHs

Levels of PAHs varied in aerosol samples between 42.82 and 270.7 pg m^{-3}, with the highest amount observed in sample 2 (Fig. 1), collected in the Southern Ocean after 59° of South latitude and in the Ross Sea, followed by samples 3 and 4, both collected in the Ross Sea. The lowest PAH content was detected in sample 1, collected before the Antarctic convergence area, from the New Zealand coasts until 59° of South latitude. The most abundant PAHs were BBF (44.61–91.54 pg m^{-3}), CRY (12.07–73.56 pg m^{-3}), BKF (5.084–56.63 pg m^{-3}), and BAP (16.51–38.65 pg m^{-3}). In sample 1 only three compounds (ACNY, ACN, BAP) were identified, while sample 2 showed the highest number of detected compounds, including ANT, which was present only in this sample, and levels of PHE and FLT (14.31 and 13.92 pg m^{-3}, respectively) ten times higher than the other samples. Samples 3 and 4 had a similar PAH pattern, in which the highest abundances were those of BBF (35-26%), CRY (28-12%), BKF (11–33%), and BAP (12–22%). Sample 5 showed the prevalence of BAP (34%), followed by PYR and CRY (25% both).

4. Discussion

4.1. Biomass burning as a source of aerosol in the ross sea

Australian wildfires taking place in summer 2019–2020 had local and global consequences, and several observations regarding fire smoke transport and distribution have been already reported. At the end of December 2019, smoke was injected in the stratosphere due to several pyrocumulonimbus events (Kablick et al., 2020). Wildfire smoke travelled 11,000 km reaching South America in January 2020 (Ohneiser et al., 2020) and phytoplankton blooms were observed in the Southern Ocean as a consequence of smoke fertilization (Tang et al., 2021). From the end of January, the stratospheric injection of smoke from Australian Black Summer was observed for the first time at the French Antarctic station Dumont d'Urville, with increased levels of ozone and aerosol (Tencé et al., 2022). To our knowledge, the influence of Black Summer smoke in the Antarctic troposphere has not been reported yet. However, in our study, the levels of Levoglucosan resulted one order of magnitude higher than levels reported for a previous campaign in the Ross Sea (Barbaro et al., 2015) and in the Antarctic coastal area at Campo Faraglione (Zangrando et al., 2016a), and two order of magnitude higher than in another study conducted in the Ross Sea (Kim et al., 2023). Levoglucosan values observed in this study were higher than concentrations found in the Arctic region (Feltracco et al., 2020; Zangrando et al., 2013).

Assessing the glucose/levoglucosan ratio (G/L) proves valuable in gauging the influence of BB on collected aerosol. Ratios around 4.5 suggest smoke-free samples, whereas values below 0.9 are linked to samples exposed to smoke (Barbaro et al., 2015; Medeiros et al., 2006a; Samburova et al., 2013; Zangrando et al., 2016b). In this study, G/L resulted <0.9 in all samples, suggesting that one of the main sources of glucose was BB, although its biogenic input may always be present. Levoglucosan showed a good correlation with the other anydrosugars mannosan (R^2 = 0.73) and galactosan (R^2 = 0.79), therefore the ratio among these sugars can help in the identification of type of biomass burned. The levoglucosan/mannosan ratio (L/M) ranged between 24 and 61, with a mean value of 39. L/M values are known to be quite variables (Fabbri et al., 2009). In Austria values of 3.6–3.9 were reported for softwood BB aerosol, while values of 14.5–14.6 were associated to hardwoods (Schmidl et al., 2008). Other authors reported higher values (13–24, 13.8–32.3) for hardwood burning (Engling et al., 2006; Fine et al., 2004). Different L/M values are generally reported for the burning of grass (2–35) (Iinuma et al., 2007; Oros et al., 2006) and shrublands (3.9–73.9) (Garcia-Hurtado et al., 2014), while the ratios associated to crop residues ranges between 12 and 55 (Oros et al., 2006; Zhang et al., 2007). Australian Black Summer is known to have burned primarily large hardwood Eucalyptus forest regions, together with savanna, shrublands, grasslands and plantations (Davey and Sarre, 2020; Levin et al., 2021). The L/M values observed in our study agrees with literature values and could represent a mixed source of hardwood and savanna. This fact could also explain the high L/M detected in this study. Similar ratios of 28–34 were observed in Australian aerosol collected in Brisbane in 2011 (He et al., 2016) during open wildfire season,
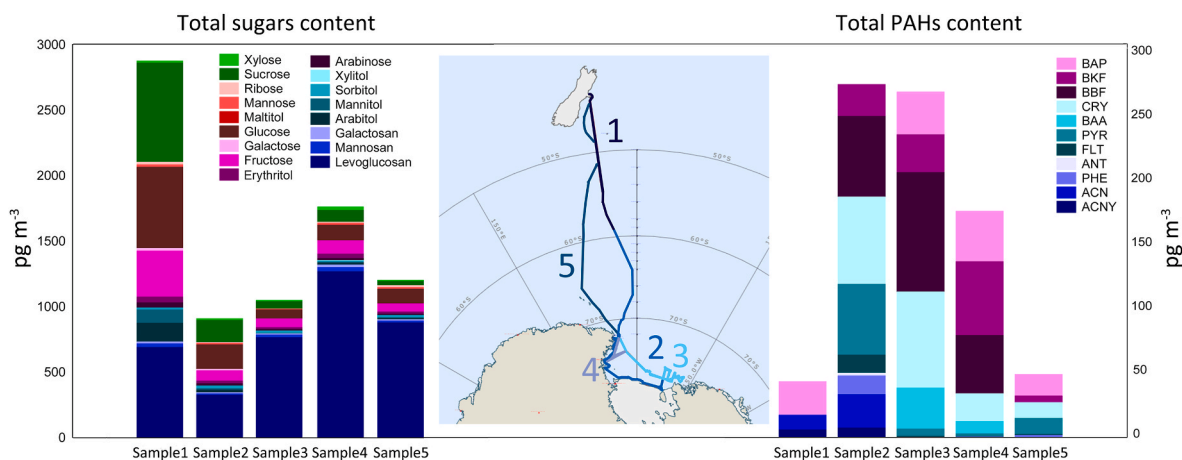

Fig. 1. Concentrations of sugars and polycyclic aromatic hydrocarbons (PAHs) in aerosol samples and sailing route of the R/V Laura Bassi during the XXXV Italian Antarctic Expedition, showing the sampling routes (MY WAY application, myway.enea.it). ACNY: acenaphthylene; ACN: acenaphthene; PHE: phenanthrene; ANT: anthracene; FLT: fluoranthene; PYR: pyrene; BAA: benz[*a*]anthracene; CRY: chrysene; BBF: benzo[*b*]fluoranthene; BKF: benzo[*k*]fluoranthene; BAP: benzo[*a*]pyrene.

attributable to the prescribed burning of agricultural residues.

Interestingly, anhydrosugars showed no significant (p value < 0.05) correlation with PAHs, excepting BAP ($R^2 = 0.83$) and a weak relation with BKF ($R^2 = 0.55$). Total PAH levels detected in this work (42.82–270.7 pg m^{-3}) were similar to concentrations reported for the Ross Sea area (near the Mario Zucchelli Italian station) during the VI (16–689 pg m^{-3}), VII (23–663 pg m^{-3}), and VIII (14–256 pg m^{-3}) Italian Antarctic expeditions (Caricchia et al., 1993, 1995). Total PAH content in our study was also in the range of concentrations (21–328 pg m^{-3}) reported by Piazza et al. (2013) in the same study area. Slightly higher levels (420–6760, 80–2010 pg m^{-3}) were instead reported for marine aerosol collected around the Antarctic Peninsula (Cabrerizo et al., 2014). However, our samples resulted particularly enriched in BAP, with a mean concentration of 22.72 pg m^{-3}, in comparison to mean values of 9, 9, and 6 pg m^{-3} reported respectively for the VI,VII, and VIII Italian Antarctic expeditions (Caricchia et al., 1995). Still in the Terra Nova Bay, Piazza et al. (2013) reported a maximum BAP concentration of 3 pg m^{-3}, while lower levels (0.13 pg m^{-3}) were observed by Barbaro et al. (2016a). The same general enrichment was observed for BKF (mean of 23.03 pg m^{-3}) and BBF (39.61 pg m^{-3}); the mean detected concentrations for the sum of BBF, BKF, and BJF (Benzo[j]fluoranthene) during the VI, VII, and VIII Italian Antarctic expeditions were 18, 34, and 26 pg m^{-3}, respectively (Caricchia et al., 1993, 1995). In addition, also BAA and CRY showed slightly higher mean values (8.20 and 34.78 pg m^{-3}) in this study than in the mentioned previous ones. These findings could suggest a mixed source for PAHs in aerosol samples, both in relation to Australian Black Summer fires and other regional sources. BPER and IPYR concentrations below the detection limits in all samples suggest that gas/oil combustion is not the main PAH source, as previously indicated for the same study area (Caricchia et al., 1995).

4.2. Monosaccharides as marker of marine primary productivity

It is interesting to note that the samples collected in the area near New Zealand and Australia showed the lowest contribution of BB tracers, indicating the predominance of other aerosol sources. The investigation of the biogenic aerosol sources present in the region is important to help the interpretation of BB signal in the collected samples and to better understand processes involved in aerosol formation and transport mechanism in Antarctica region. While the BB indicators were the dominant sugars in samples 3, 4, and 5, indeed, similar contributions of anhydrosugars and monosaccharides were detected in samples 1 and 2. The relative abundances of monosaccharides in samples 1 and 2 were 35 and 37%, respectively, those of anhydrosugars 25–37%. In both samples, high levels of sucrose were also detected, with a relative contribution of 26 and 18%, respectively. The dominant monosaccharides in samples 1 and 2 were fructose and glucose, which showed high correlation ($R^2 = 0.99$) between them and with sucrose ($R^2 = 0.99$). These three compounds were also highly correlated ($R^2 > 0.98$) with two alcohol sugars (arabitol and mannitol) and with arabinose, suggesting a common source for this group of compounds. Concentrations of monosaccharides and alcohol sugars (165–1082 pg m^{-3}, 35–303 pg m^{-3}) were in agreement with those reported in a previous campaign in the same area (374–1356 pg m^{-3}, 3–444 pg m^{-3}) (Barbaro et al., 2015) and higher than monosaccharides detected in another campaign in the Terra Nova Bay coastal area (70–410 pg m^{-3}) (Kim et al., 2023). Saccharide and alcohol sugar values were in agreement also with concentrations detected in the Arctic region during summer season (Feltracco et al., 2020). However, sample 1 resulted particularly enriched in Sucrose (757 pg m^{-3}) in comparison to previously reported levels. Sucrose is a key-component of higher plants and particularly related to pollen grains (Fu et al., 2012; Medeiros et al., 2006b). Increased concentrations of this disaccharide in Antarctica have been related to biological degradation of polysaccharides (Barbaro et al., 2017b), phytoplanktonic emissions (Kim et al., 2023), and terrestrial primary biological emissions (Decesari et al., 2020). High levels of sucrose (3560

pg m^{-3}) were recently detected near the New Zealand coasts, being attributed to a mixed oceanic and terrestrial source (Kim et al., 2023). Considering also backward trajectories (Fig. S1), the high saccharide levels found in sample 1 can be influenced both by terrestrial sources, related to air masses deriving from New Zealand and Australia, and marine sources, in relation to phytoplanktonic and algal presence. While glucose has been related also to BB sources (Medeiros et al., 2006a), fructose is more specific of biogenic ones and, in polar and marine areas, it has been related to pollens and vegetation (Yttri et al., 2007) and to the degradation of polysaccharides occurred during LRAT (Barbaro et al., 2017a, 2017b). In remote marine aerosol, Chen et al. (2013) attributed to fructose, glucose, arabitol, and mannitol a common mixed source from fungal spores and growing plants. The high correlation between arabitol and arabinose can indicate bacterial or fungal activity, since the metabolism of these sugars is well known in these organisms (Feltracco et al., 2020). Mannitol is common in plants and algae (Burshtein et al., 2011) and has a potential cryoprotectant role (Weinstein et al., 1997) in fungal spores. The detected levels of arabitol and mannitol can be related both to marine sources, releasing these compounds *via* bubble bursting processes at the sea surface (Deng et al., 2021), and to terrestrial sources (Fu et al., 2012).

To support aerosol source identification, the presence of carboxylic acids and their diagnostic ratios were evaluated. Important sources of carboxylic acids can be secondary organic aerosol (SOA) formation (Kawamura and Bikkina, 2016), fossil fuel combustion (Kawamura et al., 2000; Wang et al., 2006), and marine emissions (Fu et al., 2013). The C_3/C_4 ratio was evaluated as an indicator of aerosol photochemical oxidation, since C_4-succinic acid can be degraded to C_3-malonic acid. In this study, this ratio ranged from 2.2 to 5, with the highest value detected in sample 1, and was consistent with previous findings (Fu et al., 2013) indicating higher C_3/C_4 ratios in marine areas in comparison to urban regions. Indeed, the C_3/C_4 ratio for vehicular exhausts is usually lower (0.25–0.44) (Hegde and Kawamura, 2012) while in the Southern Ocean mean values of 1.6–1.7 have been reported (Barbaro et al., 2016a; Fu et al., 2013). Two sources of C_3-malonic acid has been suggested: 1) the photochemical production during LRAT from continents and 2) the volatilization of biological malonic acid by bubble bursting in open ocean (Aggarwal and Kawamura, 2009; Barbaro et al., 2016a). The C_4 M/F ratio (*cis*-C_4-maleic/*trans*-C_4-fumaric acids) was also evaluated, ranging from 0.46 to 1.6, with the highest value detected in sample 1. Our results are in agreement with values reported for marine areas (0.1–1.5) (Fu et al., 2013); slightly higher values are generally reported in urban regions (0.9–2.3) since *cis*-maleic acid can derive from the photochemical oxidation of benzene or toluene in urban areas, near their emission sources. The presence of *trans*-fumaric acid can suggest non-anthropogenic precursors (Kawamura et al., 1996) of this compound, such as phenolic compounds from macroalgae from sea-surface slicks (Barbaro et al., 2016a; Carlson, 1982). In general, high C_4 M/F ratios indicate less photochemical activity while lower values indicate air masses aging processes (Kawamura and Bikkina, 2016). This finding supports the major primary aerosol contribution in sample 1, which had the highest C_3/C_4 and C_4 M/F ratios, probably with the major marine aerosol contribution.

Also chloride depletion calculation can help in the evaluation of sea-spray aerosol aging, since during transport the reaction of sodium chloride with acid species (*e.g.*, sulfuric, nitric or organic acids) releases hydrochloric acid in the atmosphere (Su et al., 2022). This phenomenon is more pronounced during summer (Teinilä et al., 2014), in presence of anthropogenic pollution (Virkkula et al., 2006), and more evident in sub-micrometer particles (Barbaro et al., 2019). In this study, chloride depletion ranged between 29 and 35% in all samples excepting sample 3, which showed a value of 75%, suggesting a higher contribution of aged aerosol deriving from LRAT in comparison to the other samples.

4.3. Main aerosol sources in the ross sea

HCA was carried out to identify the main sources of aerosol. Na^+, K^+, Ca^{2+}, SO_4^{2-}, and MSA were introduced in the data matrix to support the identification of the specific aerosol sources and ionic source apportionment has been calculated as already described by (Udisti et al., 2016). The sea-salt (ss) and no-sea-salt (nss) portions of Na^+, K^+, and Ca^{2+} have been calculated. The sea-salt ($ssSO_4^{2-}$), crustal ($crSO_4^{2-}$) and anthropogenic ($antrSO_4^{2-}$) contributions to total sulfate were also evaluated. The $ssSO_4^{2-}$ was calculated considering ss-Na^+ as a sea spray marker with a 0.253 SO_4^{2-}/Na^+ w/w ratio in seawater. The non-sea-salt fraction of sulfate ($nssSO_4^{2-}$) was subtracted by the tot-SO_4^{2-} concentration and the contributions of $crSO_4^{2-}$ ($SO_4^{2-}/Ca^{2+} = 0.59$ w/w ratio) and $antrSO_4^{2-}$ (as residual fraction after $bioSO_4^{2-}$ subtraction) were estimated. Bio-SO_4^{2-} was calculated considering SO_4^{2-}/MSA ratio = 3 in biogenic aerosol in polar regions and was not included in the HCA since it was considered a repetition of MSA.

The HCA showed the presence of three main clusters of analyzed compounds that can be related to three different aerosol sources (Fig. 2).

The first cluster includes the ionic indicators of sea spray presence ($ssCa^{2+}$, $ssSO_4^{2-}$, $ssNa^+$, ssK^+) together with the monosaccharides (ribose, mannose, galactose, glucose, arabinose, fructose), the disaccharide sucrose, and three alcohol sugars (erythritol, mannitol, arabitol). This group is clearly related to biogenic aerosol sources and particularly to marine air masses, probably predominant in comparison to terrestrial sources, especially in sample 1, in which these compounds showed the highest contribution.

The second cluster includes the anhydrosugars, highly related to BAP and BKF and to the sugars xylose, maltitol, and xylitol. xylose is the main component of the xylan hemicellulose and is present in hardwood and softwood, while maltitol is a sugar alcohol derived from maltose, the main sugar in crops. It is possible that xylose and maltitol are subproduct of BB during Australian wildfires. Indeed, xylose has already been related to BB sources (Ren et al., 2020). Xylitol has been found in BB aerosol (Gao et al., 2003) and it is widely detected during particulate matter monitoring studies (Nirmalkar et al., 2015; Ren et al., 2020; Theodosi et al., 2018). Although less related to the previously described compounds, in the same cluster are present the PAHs with four and five aromatic rings BBF, CRY, and BAA, together with the anthropogenic
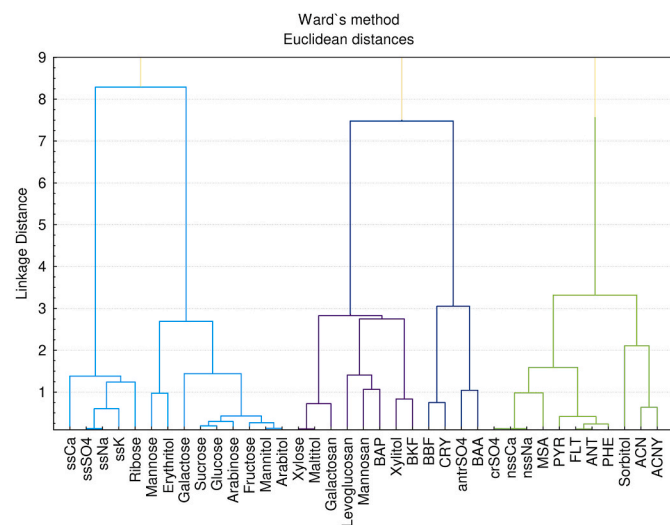
fraction of SO_4^{2-}. The presence of PAHs in aerosol generated by wildfires has been widely assessed (Campos and Abrantes, 2021; Wang et al., 2017; Yuan et al., 2008); considering their diagnostic parameters, the predominance of high molecular weight PAHs (>4 aromatic rings) generally indicate combustion sources, while high levels of low molecular weight PAHs (2–3 rings) are more related to petrogenic sources (Kieta et al., 2023). Moreover, a ratio BAA/(BAA + CRY) < 0.35 in samples 3 and 4 indicate the influence of combustion of wood or grass (Kieta et al., 2023) while the other samples seem to be more related to petrogenic sources. Recently, Zhang et al., 2021 indicated wood combustion from Australia as a major source for BBF and CRY levels detected in the Southern Ocean and Antarctic aerosol. Looking to backward trajectories of sample 3 (Fig. S2), performed considering a LRAT of 168 h, it is clear that part of aerosol was coming from Antarctic Peninsula, near South America. This is in agreement with the studies highlighting that the Australian wildfire smoke travelled mainly eastward and southward, reaching South America (Ohneiser et al., 2020) and being then transported in high stratosphere over the western coast of Antarctica (Tencé et al., 2022).

The third cluster includes compounds related to different sources: the 3–4 ring PAHs (PYR, FLT, ANT, PHE, ACN, ACNY), the crustal indicators $crSO_4^{2-}$ together with $nssCa^{2+}$ and $nssNa^+$, and MSA which is a phytoplanktonic emission tracer (Becagli et al., 2022). PAHs in this group are highly correlated ($R^2 > 0.98$) while having no correlation with the other hydrocarbons, thus indicating different aerosol sources for this class of contaminants. Levels of ACN, PHE, ANT, FLT, and PYR in aerosol have recently been related to coal combustion sources in the Southern Ocean, deriving from Australia and the Indian Ocean ship traffic (Zhang et al., 2021). These PAHs showed the highest levels in sample 2, collected after the Antarctic convergence area and in the Ross Sea. Observing the backward trajectories (Fig. S3) of sample 2, performed at the starting, intermediate and final points of ship sampling route, overlayed with Chlorophyll-*a* data for the same period, it is clear the contribution of air masses deriving from Southern Ocean, together with its phytoplanktonic activity, and from coastal and hinterland areas (crustal indicators). The volatilization of 3-ring biogenic PAHs from reservoirs in soils and snow has also been suggested as a source of these compounds in the gas-phase during austral summer in the Antarctic Peninsula (Cabrerizo et al., 2014). The presence of different aerosol sources in the air masses collected in sample 2 could explain the correlation among different tracers. Sorbitol, the only sugar present in this cluster, has been candidate as a tracer of soil dust resuspension (Simoneit et al., 2004).

5. Conclusions

In this work the analysis of aerosol samples collected in the Southern Ocean and in the Ross Sea during the 2019–2020 austral summer, at the end of the Australian Black Summer wildfires, is reported. The content of different tracers of aerosol is evaluated: levoglucosan as marker of BB, primary and alcohol sugars as indicators of biogenic emissions, and PAHs, which are related both to anthropogenic activities and BB emissions. Results indicate the contribution of smoke, especially in sample 3 and in the other samples collected in the Ross Sea. This finding, together with the evaluation of backward trajectories, suggest the transport of wildfire plume until South America and then entering the Antarctic atmosphere, in agreement with literature (Ohneiser et al., 2020; Tencé et al., 2022). The high levoglucosan concentrations observed during all the campaign indicate the widespread presence of smoke in this region, probably in relation to the stratospheric persistence of the plume over Antarctica (Kablick et al., 2020). As reported by the IPCC, 2021, a medium confidence is associated to the higher probability of fire-promoting weather conditions occurrence in Australia over the last century. Modelling studies indicate that fire weather conditions are expected to increase also in the future in Australia with high confidence (Abatzoglou et al., 2019; Abram et al., 2021; Dowdy et al., 2019). It is therefore

Fig. 2. Dendrogram of hierarchical cluster analysis on sugars, polycyclic aromatic hydrocarbons, and ions. Antr: anthropogenic; cr: crustal; nss: no-sea-salt; ss: sea-salt. MSA: methanesulfonic acid.
ACNY: acenaphthylene; ACN: acenaphthene; PHE: phenanthrene; ANT: anthracene; FLT: fluoranthene; PYR: pyrene; BAA: benz[*a*]anthracene; CRY: chrysene; BBF: benzo[*b*]fluoranthene; BKF: benzo[*k*]fluoranthene; BAP: benzo[*a*]pyrene.

crucial to strengthens the investigations on the regional climatic effects of these events in Antarctica, which could affect the albedo, direct radiative forcing, and ice nucleation processes (Flanner et al., 2007; IPCC, 2021; Ramanathan and Carmichael, 2008). PAHs showed to be only partially related to BB event, probably having different regional sources as coal combustion from ship traffic, petrogenic releases or biogenic sources (Cabrerizo et al., 2014; Zhang et al., 2021). Biogenic sources, both marine and terrestrial, have also contributed to the aerosol collected, as indicated by sugars and ionic species, and were dominant especially in the open Southern Ocean, far from Antarctic coastal area. This aspect is mainly related to the prevailing presence of BB aerosol over the Antarctic continent, in accordance with the eastward transport of smoke.

CRediT authorship contribution statement

Elisa Scalabrin: Writing – review & editing, Writing – original draft, Visualization, Funding acquisition, Data curation, Conceptualization. **Elena Barbaro:** Writing – review & editing, Writing – original draft, Validation, Methodology, Investigation, Formal analysis. **Sarah Pizzini:** Writing – review & editing, Writing – original draft, Validation, Methodology, Investigation, Formal analysis, Conceptualization. **Marta Radaelli:** Resources, Project administration, Funding acquisition, Conceptualization. **Matteo Feltracco:** Writing – review & editing, Validation, Methodology, Investigation, Formal analysis. **Rossano Piazza:** Writing – review & editing, Supervision, Funding acquisition. **Andrea Gambaro:** Writing – review & editing, Supervision, Funding acquisition. **Gabriele Capodaglio:** Writing – review & editing, Writing – original draft, Supervision, Funding acquisition, Conceptualization.

Declaration of competing interest

The authors declare that they have no known competing financial interests or personal relationships that could have appeared to influence the work reported in this paper.

Data availability

Data will be made available on request.

Acknowledgements

Appendix A. sSupplementary data

Supplementary data to this article can be found online at https://doi.org/10.1016/j.chemosphere.2024.142073.

References

Abatzoglou, J.T., Williams, A.P., Barbero, R., 2019. Global emergence of anthropogenic climate change in fire weather indices. Geophys. Res. Lett. 46, 326–336. https://doi.org/10.1029/2018GL080959.

Abram, N.J., Henley, B.J., Gupta, A. Sen, Lippmann, T.J.R., Clarke, H., Dowdy, A.J., Sharples, J.J., Nolan, R.H., Zhang, T., Wooster, M.J., Wurtzel, J.B., Meissner, K.J., Pitman, A.J., Ukkola, A.M., Murphy, B.P., Tapper, N.J., Boer, M.M., 2021. Connections of climate change and variability to large and extreme forest fires in southeast Australia. Commun. Earth Environ. 2 https://doi.org/10.1038/s43247-020-00065-8.

Aggarwal, S.G., Kawamura, K., 2009. Carbonaceous and inorganic composition in long-range transported aerosols over northern Japan: implication for aging of water-soluble organic fraction. Atmos. Environ. 43, 2532–2540. https://doi.org/10.1016/j.atmosenv.2009.02.032.

Barbaro, E., Feltracco, M., Cesari, D., Padoan, S., Zangrando, R., Contini, D., Barbante, C., Gambaro, A., 2019. Characterization of the water soluble fraction in ultrafine, fine,

and coarse atmospheric aerosol. Sci. Total Environ. 658, 1423–1439. https://doi.org/10.1016/j.scitotenv.2018.12.298.

Barbaro, E., Kirchgeorg, T., Zangrando, R., Vecchiato, M., Piazza, R., Barbante, C., Gambaro, A., 2015. Sugars in Antarctic aerosol. Atmos. Environ. 118, 135–144. https://doi.org/10.1016/j.atmosenv.2015.07.047.

Barbaro, E., Morabito, E., Gregoris, E., Feltracco, M., Gabrieli, J., Vardè, M., Cairns, W.R. L., Dallo, F., De Blasi, F., Zangrando, R., Barbante, C., Gambaro, A., 2020. Col Margherita Observatory: A background site in the Eastern Italian Alps for investigating the chemical composition of atmospheric aerosols. Atmos. Environ. 221. https://doi.org/10.1016/j.atmosenv.2019.117071.

Barbaro, E., Padoan, S., Kirchgeorg, T., Zangrando, R., Toscano, G., Barbante, C., Gambaro, A., 2017a. Particle size distribution of inorganic and organic ions in coastal and inland Antarctic aerosol. Environ. Sci. Pollut. Res. 24, 2724–2733. https://doi.org/10.1007/s11356-016-8042-x.

Barbaro, E., Zangrando, R., Kirchgeorg, T., Bazzano, A., Illuminati, S., Annibaldi, A., Rella, S., Truzzi, C., Grotti, M., Ceccarini, A., Malitesta, C., Scarponi, G., Gambaro, A., 2016a. An integrated study of the chemical composition of Antarctic aerosol to investigate natural and anthropogenic sources. Environ. Chem. 13, 867–876. https://doi.org/10.1071/EN16056.

Barbaro, E., Zangrando, R., Padoan, S., Karroca, O., Toscano, G., Cairns, W.R.L., Barbante, C., Gambaro, A., 2017b. Aerosol and snow transfer processes: An investigation on the behavior of water-soluble organic compounds and ionic species. Chemosphere 183, 132–138. https://doi.org/10.1016/j.chemosphere.2017.05.098.

Becagli, S., Barbaro, E., Bonamano, S., Caiazzo, L., Di Sarra, A., Feltracco, M., Grigioni, P., Heintzenberg, J., Lazzara, L., Legrand, M., Madonia, A., Marcelli, M., Melillo, C., Meloni, D., Nuccio, C., Pace, G., Park, K.T., Preunkert, S., Severi, M., Vecchiato, M., Zangrando, R., Traversi, R., 2022. Factors controlling atmospheric DMS and its oxidation products (MSA and nssSO42-) in the aerosol at Terra Nova Bay, Antarctica. Atmos. Chem. Phys. 22, 9245–9263. https://doi.org/10.5194/acp-22-9245-2022.

Bowman, D., Williamson, G., Yebra, M., Lizundia-Loiola, J., Pettinari, M.L., Shah, S., Bradstock, R., Chuvieco, E., 2020. Wildfires: Australia needs national monitoring agency. Nature 584, 188–191. https://doi.org/10.1038/d41586-020-02306-4.

Burshtein, N., Lang-Yona, N., Rudich, Y., 2011. Ergosterol, arabitol and mannitol as tracers for biogenic aerosols in the eastern Mediterranean. Atmos. Chem. Phys. 11, 829–839. https://doi.org/10.5194/acp-11-829-2011.

Cabrerizo, A., Galbán-Malagón, C., Vento, S. Del, Dachs, J., 2014. Sources and fate of polycyclic aromatic hydrocarbons in the Antarctic and Southern Ocean atmosphere. Global Biogeochem. Cycles 28, 1424–1436. https://doi.org/10.1002/2014GB004910.

Campos, I., Abrantes, N., 2021. Forest fires as drivers of contamination of polycyclic aromatic hydrocarbons to the terrestrial and aquatic ecosystems. Curr. Opin. Environ. Sci. Heal. 24, 100293 https://doi.org/10.1016/j.coesh.2021.100293.

Canadell, J.G., Meyer, C.P., Mick, Cook, G.D., Dowdy, A., Briggs, P.R., Knauer, J., Pepler, A., Haverd, V., 2021. Multi-decadal increase of forest burned area in Australia is linked to climate change. Nat. Commun. 12 https://doi.org/10.1038/s41467-021-27225-4.

Cao, S., Na, G., Li, R., Ge, L., Gao, H., Jin, S., Hou, C., Gao, Y., Zhang, Z., 2018. Fate and deposition of polycyclic aromatic hydrocarbons in the Bransfield Strait, Antarctica. Mar. Pollut. Bull. 137, 533–541. https://doi.org/10.1016/j.marpolbul.2018.10.045.

Caricchia, A.M., Chiavarini, S., Cremisini, C., Fantini, M., Morabito, R., Perini, A., Pezza, M., 1993. PAHs in atmospheric particulate in the area of Italian scientific base in Antarctica. Water Sci. Technol. 27, 235–243. https://doi.org/10.2166/wst.1993.0556.

Caricchia, A.M., Chiavarini, S., Cremisini, C., Morabito, R., Perini, A., Pezza, M., 1995. Determination of PAH in atmospheric particulates in the area of the Italian base in Antarctica: report on monitoring activities during the last three scientific expeditions. Environ. Pollut. 87, 345–356. https://doi.org/10.1016/0269-7491(94)P4166-L.

Carlson, D.J., 1982. Surface microlayer phenolic enrichment indicate sea surface slicks. Nature 296, 426–429.

Carmichael, G.R., Adhikary, B., Kulkarni, S., D'Allura, A., Tang, Y., Streets, D., Zhang, Q., Bond, T.C., Ramanathan, V., Jamroensan, A., Marrapu, P., 2009. Asian aerosols: current and year 2030 distributions and implications to human health and regional climate change. Environ. Sci. Technol. 43, 5811–5817. https://doi.org/10.1021/es8036803.

Chen, J., Kawamura, K., Liu, C.Q., Fu, P., 2013. Long-term observations of saccharides in remote marine aerosols from the western North Pacific: a comparison between 1990-1993 and 2006-2009 periods. Atmos. Environ. 67, 448–458. https://doi.org/10.1016/j.atmosenv.2012.11.014.

Cheng, Y., Engling, G., He, K.B., Duan, F.K., Ma, Y.L., Du, Z.Y., Liu, J.M., Zheng, M., Weber, R.J., 2013. Biomass burning contribution to Beijing aerosol. Atmos. Chem. Phys. 13, 7765–7781. https://doi.org/10.5194/acp-13-7765-2013.

Damany-Pearce, L., Johnson, B., Wells, A., Osborne, M., Allan, J., Belcher, C., Jones, A., Haywood, J., 2022. Australian wildfires cause the largest stratospheric warming since Pinatubo and extends the lifetime of the Antarctic ozone hole. Sci. Rep. 12, 1–15. https://doi.org/10.1038/s41598-022-15794-3.

Davey, S.M., Sarre, A., 2020. Editorial: the 2019/20 black summer bushfires. Aust. For. 83, 47–51. https://doi.org/10.1080/00049158.2020.1769899.

Decesari, S., Paglione, M., Rinaldi, M., Dall'osto, M., Simó, R., Zanca, N., Volpi, F., Cristina Facchini, M., Hoffmann, T., Götz, S., Johannes Kampf, C., O'Dowd, C., Ceburnis, D., Ovadnevaite, J., Tagliavini, E., 2020. Shipborne measurements of Antarctic submicron organic aerosols: an NMR perspective linking multiple sources and bioregions. Atmos. Chem. Phys. 20, 4193–4207. https://doi.org/10.5194/acp-20-4193-2020.

Deng, J., Gao, Y., Zhu, J., Li, L., Yu, S., Kawamura, K., Fu, P., 2021. Molecular markers for fungal spores and biogenic SOA over the Antarctic Peninsula: field measurements and modeling results. Sci. Total Environ. 762, 143089 https://doi.org/10.1016/j.scitotenv.2020.143089.

Dowdy, A.J., Ye, H., Pepler, A., Thatcher, M., Osbrough, S.L., Evans, J.P., Di Virgilio, G., McCarthy, N., 2019. Future changes in extreme weather and pyroconvection risk factors for Australian wildfires. Sci. Rep. 9, 1–11. https://doi.org/10.1038/s41598-019-46362-x.

Engling, G., Carrico, C.M., Kreidenweis, S.M., Collett, J.L., Day, D.E., Malm, W.C., Lincoln, E., Min Hao, W., Iinuma, Y., Herrmann, H., 2006. Determination of levoglucosan in biomass combustion aerosol by high-performance anion-exchange chromatography with pulsed amperometric detection. Atmos. Environ. 40, 299–311. https://doi.org/10.1016/j.atmosenv.2005.12.069.

Fabbri, D., Torri, C., Simoneit, B.R.T., Marynowski, L., Rushdi, A.I., Fabiańska, M.J., 2009. Levoglucosan and other cellulose and lignin markers in emissions from burning of Miocene lignites. Atmos. Environ. 43, 2286–2295. https://doi.org/10.1016/j.atmosenv.2009.01.030.

Feltracco, M., Barbaro, E., Tedeschi, S., Spolaor, A., Turetta, C., Vecchiato, M., Morabito, E., Zangrando, R., Barbante, C., Gambaro, A., 2020. Interannual variability of sugars in Arctic aerosol: Biomass burning and biogenic inputs. Sci. Total Environ. 706, 136089. https://doi.org/10.1016/j.scitotenv.2019.136089.

Fine, P.M., Cass, G.R., Simoneit, B.R.T., 2004. Chemical characterization of fine particle emissions from the wood stove combustion of prevalent United States tree species. Environ. Eng. Sci. 21, 705–721. https://doi.org/10.1089/ees.2004.21.705.

Flanner, M.G., Zender, C.S., Randerson, J.T., Rasch, P.J., 2007. Present-day climate forcing and response from black carbon in snow. J. Geophys. Res. Atmos. 112, 1–17. https://doi.org/10.1029/2006JD008003.

Fu, P., Kawamura, K., Barrie, L.A., 2009. Photochemical and other sources of organic compounds in the Canadian high arctic aerosol pollution during. Arctic 43, 286–292.

Fu, P., Kawamura, K., Kobayashi, M., Simoneit, B.R.T., 2012. Seasonal variations of sugars in atmospheric particulate matter from Gosan, Jeju island: significant contributions of airborne pollen and Asian dust in spring. Atmos. Environ. 55, 234–239. https://doi.org/10.1016/j.atmosenv.2012.02.061.

Fu, P., Kawamura, K., Usukura, K., Miura, K., 2013. Dicarboxylic acids, ketocarboxylic acids and glyoxal in the marine aerosols collected during a round-the-world cruise. Mar. Chem. 148, 22–32. https://doi.org/10.1016/j.marchem.2012.11.002.

Gao, S., Hegg, D.A., Hobbs, P.V., Kirschstetter, T.W., Magi, B.I., Sadilek, M., 2003. Water-soluble organic components in aerosols associated with savanna fires in southern Africa: idenification, evolution, and distribution. J. Geophys. Res. Atmos. 108 https://doi.org/10.1029/2002jd002324.

Garcia-Hurtado, E., Pey, J., Borrás, E., Sánchez, P., Vera, T., Carratalá, A., Alastuey, A., Querol, X., Vallejo, V.R., 2014. Atmospheric PM and volatile organic compounds released from Mediterranean shrubland wildfires. Atmos. Environ. 89, 85–92. https://doi.org/10.1016/j.atmosenv.2014.02.016.

He, C., Miljevic, B., Crilley, L.R., Surawski, N.C., Bartsch, J., Salimi, F., Uhde, E., Schnelle-Kreis, J., Orasche, J., Ristovski, Z., Ayoko, G.A., Zimmermann, R., Morawska, L., 2016. Characterisation of the impact of open biomass burning on urban air quality in Brisbane, Australia. Environ. Int. 91, 230–242. https://doi.org/10.1016/j.envint.2016.02.030.

Hegde, P., Kawamura, K., 2012. Seasonal variations of water-soluble organic carbon, dicarboxylic acids, ketocarboxylic acids, and α-dicarbonyls in Central Himalayan aerosols. Atmos. Chem. Phys. 12, 6645–6665. https://doi.org/10.5194/acp-12-6645-2012.

Hu, Q.H., Xie, Z.Q., Wang, X.M., Kang, H., Zhang, P., 2013. Levoglucosan indicates high levels of biomass burning aerosols over oceans from the Arctic to Antarctic. Sci. Rep. 3, 1–7. https://doi.org/10.1038/srep03119.

Iinuma, Y., Brüggemann, E., Gnauk, T., Müller, K., Andreae, M.O., Helas, G., Parmar, R., Herrmann, H., 2007. Source characterization of biomass burning particles: the combustion of selected European conifers, African hardwood, savanna grass, and German and Indonesian peat. J. Geophys. Res. Atmos. 112 https://doi.org/10.1029/2006JD007120.

IPCC, 2021. Climate change 2021 – the physical science basis. Climate Change 2021 – The Physical Science Basis. https://doi.org/10.1017/9781009157896.

Jager, H.I., Coutant, C.C., 2020. Knitting while Australia burns. Nat. Clim. Change 10, 170. https://doi.org/10.1038/s41558-020-0710-7.

Jain, P., Castellanos-Acuna, D., Coogan, S.C.P., Abatzoglou, J.T., Flannigan, M.D., 2022. Observed increases in extreme fire weather driven by atmospheric humidity and temperature. Nat. Clim. Change 12, 63–70. https://doi.org/10.1038/s41558-021-01224-1.

Jumelet, J., Klekociuk, A.R., Alexander, S.P., Bekki, S., Hauchecorne, A., Vernier, J.P., Fromm, M., Keckhut, P., 2020. Detection of aerosols in Antarctica from long-range transport of the 2009 Australian wildfires. J. Geophys. Res. Atmos. 125, 1–17. https://doi.org/10.1029/2020JD032542.

Kablick, G.P., Allen, D.R., Fromm, M.D., Nedoluha, G.E., 2020. Australian PyroCb smoke generates synoptic-scale stratospheric anticyclones. Geophys. Res. Lett. 47 https://doi.org/10.1029/2020GL088101.

Kawamura, K., Bikkina, S., 2016. A review of dicarboxylic acids and related compounds in atmospheric aerosols: molecular distributions, sources and transformation. Atmos. Res. 170, 140–160. https://doi.org/10.1016/j.atmosres.2015.11.018.

Kawamura, K., Kasukabe, H., Barrie, L.A., 1996. Source and reaction pathways of dicarboxylic acids, ketoacids and dicarbonyls in arctic aerosols: one year of observations. Atmos. Environ. 30, 1709–1722. https://doi.org/10.1016/1352-2310(95)00395-9.

Kawamura, K., Steinberg, S., Kaplan, I.R., 2000. Homologous series of C 1-C 10 monocarboxylic acids and C 1 -C 6 carbonyls in Los Angeles air and motor vehicle exhausts. Atmos. Environ. 34, 4175–4191.

Khan, S.J., 2021. Ecological consequences of Australian "Black Summer" (2019–20) fires: a synthesis of Australian Commonwealth Government report findings. Integrated Environ. Assess. Manag. 17, 1136–1140. https://doi.org/10.1002/ieam.4469.

Kieta, K.A., Owens, P.N., Petticrew, E.L., French, T.D., Koiter, A.J., Rutherford, P.M., 2023. Polycyclic aromatic hydrocarbons in terrestrial and aquatic environments following wildfire: a review. Environ. Rev. 31, 141–167. https://doi.org/10.1139/er-2022-0055.

Kim, K.A., Choi, N.R., Yoo, H.Y., Jang, E., Yoon, Y.J., Park, J., Jung, C.H., Kim, Y.P., Park, K.T., Lee, J.Y., 2023. Atmospheric saccharide composition and its possible linkage with marine phytoplankton from North Pacific to the Antarctic regions. Atmos. Environ. 292, 119420 https://doi.org/10.1016/j.atmosenv.2022.119420.

Levin, N., Yebra, M., Phinn, S., 2021. Unveiling the factors responsible for Australia's black summer fires of 2019/2020. Fire 4. https://doi.org/10.3390/fire4030058.

Medeiros, P.M., Conte, M.H., Weber, J.C., Simoneit, B.R.T., 2006a. Sugars as source indicators of biogenic organic carbon in aerosols collected above the Howland Experimental Forest, Maine. Atmos. Environ. 40, 1694–1705. https://doi.org/10.1016/j.atmosenv.2005.11.001.

Medeiros, P.M., Fernandes, M.F., Dick, R.P., Simoneit, B.R.T., 2006b. Seasonal variations in sugar contents and microbial community in a ryegrass soil. Chemosphere 65, 832–839. https://doi.org/10.1016/j.chemosphere.2006.03.025.

Nirmalkar, J., Deshmukh, D.K., Deb, M.K., Tsai, Y.I., Sopajaree, K., 2015. Mass loading and episodic variation of molecular markers in PM2.5 aerosols over a rural area in eastern central India. Atmos. Environ. 117, 41–50. https://doi.org/10.1016/j.atmosenv.2015.07.003.

Novakov, T., Corrigan, C.E., 1996. Cloud condensation nucleus activity of the organic component of biomass smoke particles. Geophys. Res. Lett. 23, 2141–2144. https://doi.org/10.1029/96GL01971.

Ohneiser, K., Ansmann, A., Baars, H., Seifert, P., Barja, B., Jimenez, C., Radenz, M., Teisseire, A., Floutsi, A., Haarig, M., Foth, A., Chudnovsky, A., Engelmann, R., Zamorano, F., Buhl, J., Wandinger, U., 2020. Smoke of extreme Australian bushfires observed in the stratosphere over Punta Arenas, Chile, in January 2020: optical thickness, lidar ratios, and depolarization ratios at 355 and 532 nm. Atmos. Chem. Phys. 20, 8003–8015. https://doi.org/10.5194/acp-20-8003-2020.

Oros, D.R., Simoneit, B.R.T., 2001. Identification and emission factors of molecular tracers in organic aerosols from biomass burning Part 1. Temperate climate conifers. Appl. Geochem. https://doi.org/10.1016/S0883-2927(01)00021-X.

Oros, D.R., Abas, M.R. bin, Omar, N.Y.M.J., Rahman, N.A., Simoneit, B.R.T., 2006. Identification and emission factors of molecular tracers in organic aerosols from biomass burning: Part 3. Grasses. Appl. Geochem. 21, 919–940. https://doi.org/10.1016/j.apgeochem.2006.01.008.

Piazza, R., Gambaro, A., Argiriadis, E., Vecchiato, M., Zambon, S., Cescon, P., Barbante, C., 2013. Development of a method for simultaneous analysis of PCDDs, PCDFs, PCBs, PBDEs, PCNs and PAHs in Antarctic air. Anal. Bioanal. Chem. 405, 917–932. https://doi.org/10.1007/s00216-012-6464-y.

Pizzini, S., Piazza, R., Cozzi, G., Barbante, C., 2016. Simultaneous determination of halogenated contaminants and polycyclic aromatic hydrocarbons: a multi-analyte method applied to filter-feeding edible organisms. Anal. Bioanal. Chem. 408, 7991–7999. https://doi.org/10.1007/s00216-016-9897-x.

Ramanathan, V., Carmichael, G., 2008. Global and regional climate changes due to black carbon. Nat. Geosci. 1, 221–227. https://doi.org/10.1038/ngeo156.

Ren, G., Yan, X., Ma, Y., Qiao, L., Chen, Z., Xin, Y., Zhou, M., Shi, Y., Zheng, K., Zhu, S., Huang, C., Li, L., 2020. Characteristics and source apportionment of PM2.5-bound saccharides and carboxylic acids in Central Shanghai, China. Atmos. Res. 237 https://doi.org/10.1016/j.atmosres.2019.104817.

Rolph, G., Stein, A., Stunder, B., 2017. Real-time environmental applications and display sYstem: ready. Environ. Model. Software 95, 210–228. https://doi.org/10.1016/j.envsoft.2017.06.025.

Ryan, R.G., Silver, J.D., Schofield, R., 2021. Air quality and health impact of 2019–20 Black Summer megafires and COVID-19 lockdown in Melbourne and Sydney, Australia. Environ. Pollut. 274 https://doi.org/10.1016/j.envpol.2021.116498.

Samburova, V., Gannet Hallar, A., Mazzoleni, L.R., Saranjampour, P., Lowenthal, D., Kohl, S.D., Zielinska, B., 2013. Composition of water-soluble organic carbon in non-urban atmospheric aerosol collected at the Storm Peak Laboratory. Environ. Chem. 10, 370–380. https://doi.org/10.1071/EN13079.

Sang, X., Zhang, Z., Chan, C., Engling, G., 2013. Source categories and contribution of biomass smoke to organic aerosol over the southeastern Tibetan Plateau. Atmos. Environ. 78, 113–123. https://doi.org/10.1016/j.atmosenv.2012.12.012.

Schmidl, C., Marr, I.L., Caseiro, A., Kotianová, P., Berner, A., Bauer, H., Kasper-Giebl, A., Puxbaum, H., 2008. Chemical characterisation of fine particle emissions from wood stove combustion of common woods growing in mid-European Alpine regions. Atmos. Environ. 42, 126–141. https://doi.org/10.1016/j.atmosenv.2007.09.028.

Shi, G., Wang, X.C., Li, Y., Trengove, R., Hu, Z., Mi, M., Li, X., Yu, J., Hunter, B., He, T., 2019. Organic tracers from biomass burning in snow from the coast to the ice sheet summit of East Antarctica. Atmos. Environ. 201, 231–241. https://doi.org/10.1016/j.atmosenv.2018.12.058.

Simmons, J.B., Paton-Walsh, C., Mouat, A.P., Kaiser, J., Humphries, R.S., Keywood, M., Griffith, D.W.T., Sutresna, A., Naylor, T., Ramirez-Gamboa, J., 2022. Bushfire smoke plume composition and toxicological assessment from the 2019–2020 Australian Black Summer. Air Qual. Atmos. Heal. 15, 2067–2089. https://doi.org/10.1007/s11869-022-01237-5.

Simoneit, B.R.T., Elias, V.O., Kobayashi, M., Kawamura, K., Rushdi, A.I., Medeiros, P.M., Rogge, W.F., Didyk, B.M., 2004. Sugars - dominant water-soluble organic compounds in soils and characterization as tracers in atmospheric participate matter. Environ. Sci. Technol. 38, 5939–5949. https://doi.org/10.1021/es0403099.

Stein, A.F., Draxler, R.R., Rolph, G.D., Stunder, B.J.B., Cohen, M.D., Ngan, F., 2015. Noaa's hysplit atmospheric transport and dispersion modeling system. Bull. Am. Meteorol. Soc. 96, 2059–2077. https://doi.org/10.1175/BAMS-D-14-00110.1.

Stohl, A., Sodemann, H., 2010. Characteristics of atmospheric transport into the Antarctic troposphere. J. Geophys. Res. Atmos. 115, 1–16. https://doi.org/10.1029/2009JD012536.

Su, B., Wang, T., Zhang, G., Liang, Y., Lv, C., Hu, Y., Li, L., Zhou, Z., Wang, X., Bi, X., 2022. A review of atmospheric aging of sea spray aerosols: potential factors affecting chloride depletion. Atmos. Environ. 290, 119365 https://doi.org/10.1016/j.atmosenv.2022.119365.

Tang, W., Llort, J., Weis, J., Perron, M.M.G., Basart, S., Li, Z., Sathyendranath, S., Jackson, T., Sanz Rodriguez, E., Proemse, B.C., Bowie, A.R., Schallenberg, C., Strutton, P.G., Matear, R., Cassar, N., 2021. Widespread phytoplankton blooms triggered by 2019–2020 Australian wildfires. Nature 597, 370–375. https://doi.org/10.1038/s41586-021-03805-8.

Teinilä, K., Frey, A., Hillamo, R., Tülp, H.C., Weller, R., 2014. A study of the sea-salt chemistry using size-segregated aerosol measurements at coastal Antarctic station Neumayer. Atmos. Environ. 96, 11–19. https://doi.org/10.1016/j.atmosenv.2014.07.025.

Tencé, F., Jumelet, J., Bekki, S., Khaykin, S., Sarkissian, A., Keckhut, P., 2022. Australian black summer smoke observed by lidar at the French antarctic station Dumont d'Urville. J. Geophys. Res. Atmos. 127, 1–16. https://doi.org/10.1029/2021JD035349.

Theodosi, C., Panagiotopoulos, C., Nouara, A., Zarmpas, P., Nicolaou, P., Violaki, K., Kanakidou, M., Sempéré, R., Mihalopoulos, N., 2018. Sugars in atmospheric aerosols over the eastern mediterranean. Prog. Oceanogr. 163, 70–81. https://doi.org/10.1016/j.pocean.2017.09.001.

Udisti, R., Bazzano, A., Becagli, S., Bolzacchini, E., Caiazzo, L., Cappelletti, D., Ferrero, L., Frosini, D., Giardi, F., Grotti, M., Lupi, A., Malandrino, M., Mazzola, M., Moroni, B., Severi, M., Traversi, R., Viola, A., Vitale, V., 2016. Sulfate source apportionment in the ny-ålesund (svalbard islands) arctic aerosol. Rend. Lincei 27, 85–94. https://doi.org/10.1007/s12210-016-0517-7.

Virkkula, A., Teinilä, K., Hillamo, R., Kerminen, V.M., Saarikoski, S., Aurela, M., Koponen, I.K., Kulmala, M., 2006. Chemical size distributions of boundary layer aerosol over the Atlantic Ocean and at an Antarctic site. J. Geophys. Res. Atmos. 111, 1–14. https://doi.org/10.1029/2004JD004958.

Wang, H., Kawamura, K., Yamazaki, K., 2006. Water-soluble dicarboxylic acids, ketoacids and dicarbonyls in the atmospheric aerosols over the Southern Ocean and Western Pacific Ocean. J. Atmos. Chem. 53, 43–61. https://doi.org/10.1007/s10874-006-1479-4.

Wang, X., Meyer, C.P., Reisen, F., Keywood, M., Thai, P.K., Hawker, D.W., Powell, J., Mueller, J.F., 2017. Emission factors for selected semivolatile organic chemicals from burning of tropical biomass fuels and estimation of annual Australian emissions. Environ. Sci. Technol. 51, 9644–9652. https://doi.org/10.1021/acs.est.7b01392.

Weinstein, R.N., Palm, M.E., Johnstone, K., Wynn-Williams, D.D., 1997. Ecological and physiological characterization of Humicola marvinii , a new psychrophilic fungus from fellfield soils in the maritime Antarctic. Mycologia 89, 706–711. https://doi.org/10.1080/00275514.1997.12026836.

Yttri, K.E., Dye, C., Kiss, G., 2007. Ambient aerosol concentrations of sugars and sugar-alcohols at four different sites in Norway. Atmos. Chem. Phys. 7, 4267–4279. https://doi.org/10.5194/acp-7-4267-2007.

Yu, P., Xu, R., Abramson, M.J., Li, S., Guo, Y., 2020. Bushfires in Australia: a serious health emergency under climate change. Lancet Planet. Health 4, e7–e8. https://doi.org/10.1016/S2542-5196(19)30267-0.

Yuan, H., Tao, S., Li, B., Lang, C., Cao, J., Coveney, R.M., 2008. Emission and outflow of polycyclic aromatic hydrocarbons from wildfires in China. Atmos. Environ. 42, 6828–6835. https://doi.org/10.1016/j.atmosenv.2008.05.033.

Zangrando, R., Barbaro, E., Kirchgeorg, T., Vecchiato, M., Scalabrin, E., Radaelli, M., Đorđević, D., Barbante, C., Gambaro, A., 2016a. Five primary sources of organic aerosols in the urban atmosphere of Belgrade (Serbia). Sci. Total Environ. 571, 1441–1453. https://doi.org/10.1016/j.scitotenv.2016.06.188.

Zangrando, R., Barbaro, E., Vecchiato, M., Kehrwald, N.M., Barbante, C., Gambaro, A., 2016b. Levoglucosan and phenols in Antarctic marine, coastal and plateau aerosols. Sci. Total Environ. 544, 606–616. https://doi.org/10.1016/j.scitotenv.2015.11.166.

Zangrando, R., Barbaro, E., Zennaro, P., Rossi, S., Kehrwald, N.M., Gabrieli, J., Barbante, C., Gambaro, A., 2013. Molecular markers of biomass burning in Arctic aerosols. Environ. Sci. Technol. 47, 8565–8574. https://doi.org/10.1021/es400125r.

Zhang, Y., xun hang xun, Shao, M., Zhang, Y., xun hang xun, Zeng, min, L., He, yan, L., Zhu, B., Wei, Y., jie, Zhu, lei, X., 2007. Source profiles of particulate organic matters emitted from cereal straw burnings. J. Environ. Sci. 19, 167–175. https://doi.org/10.1016/S1001-0742(07)60027-8.

Zhang, X.X., Zhang, Z.F., Zhang, X.X., Zhu, F.J., Li, Y.F., Cai, M., Kallenborn, R., 2021. Polycyclic aromatic hydrocarbons in the marine atmosphere from the western pacific to the Southern Ocean: spatial variability, gas/particle partitioning, and source apportionment. Environ. Sci. Technol. https://doi.org/10.1021/acs.est.1c08429.